

DTP/95/62  
July 1995

# Analytic Approaches to the Evolution of Polarised Parton Distributions at Small $x$

T. Gehrmann and W.J. Stirling

*Departments of Physics and Mathematical Sciences, University of Durham  
Durham DH1 3LE, England*

## Abstract

The  $Q^2$  evolution of polarised parton distributions at small  $x$  is studied. Various analytic approximations are critically discussed. We compare the full evolution with that obtained from the leading-pole approximation to the splitting functions, and show that the validity of this approximation depends critically on the  $x \rightarrow 0$  behaviour of the starting distributions. A new analytic solution which is valid at small  $x$  is obtained, and its domain of applicability is discussed.

# 1 Introduction

The first moment of the polarised structure function  $g_1(x, Q^2)$ , the Ellis-Jaffe sum rule [1], determines the overall spin content of the nucleon. Measurements of the Ellis-Jaffe sum rule [2, 3] involve an extrapolation of  $g_1$  for  $x \rightarrow 0$ , which is usually performed by fitting a Regge-motivated form

$$g_1(x) = Cx^\alpha \quad (1)$$

to the experimental data points with the lowest  $x$ -values. This procedure can be problematic, since these data points are usually taken at a relatively low scale of  $Q^2 \sim 1 \text{ GeV}^2$ , whereas the overall sum rule is evaluated at the average  $Q^2$  of the experiment, which is typically between 3 and 10  $\text{GeV}^2$ .

In the recent past, various authors have attempted to calculate the asymptotic behaviour of  $g_1(x)$  (see for example Ref. [4] for a review of the various approaches). At scales of low momentum transfer ( $Q^2 \approx 1 \text{ GeV}^2$ ), a non-perturbative calculation [5] of the flavour singlet contribution to  $g_1$  shows good agreement with  $g_1^p$  at small  $x$ , but it should be noted that the normalisation of this non-perturbative contribution is highly sensitive to the only approximately known value of the vacuum quark condensate. The experimental discrepancy between  $g_1^p$  and  $g_1^d$  in the small- $x$  region seems to contradict the above result. As the singlet distribution is identical for both targets, this discrepancy indicates a sizeable valence-quark contribution in this region.

With increasing  $Q^2$ , perturbative corrections become more and more important. These corrections affect both the valence and the singlet contributions ( $\Delta\Sigma = \sum_q(\Delta q + \Delta\bar{q})$ ) to  $g_1$  and give rise to an evolution of the corresponding parton densities [6]

$$\begin{aligned} \frac{\partial}{\partial \ln Q^2} \Delta q_{val}(x, Q^2) &= \int_x^1 \frac{dy}{y} \Delta P_{qq}(y) \Delta q_{val}(x/y, Q^2) \\ \frac{\partial}{\partial \ln Q^2} \begin{pmatrix} \Delta\Sigma \\ \Delta G \end{pmatrix} (x, Q^2) &= \frac{\alpha_s(Q^2)}{2\pi} \int_x^1 \frac{dy}{y} \begin{pmatrix} \Delta P_{qq} & \Delta P_{qg} \\ \Delta P_{gq} & \Delta P_{gg} \end{pmatrix} (y) \begin{pmatrix} \Delta\Sigma \\ \Delta G \end{pmatrix} (x/y, Q^2), \end{aligned} \quad (2)$$

without determining the densities themselves. These enter the above equation in the form of the initial distributions  $\Delta q_{val}(x, Q_0^2)$ ,  $\Delta\Sigma(x, Q_0^2)$  and  $\Delta G(x, Q_0^2)$ , which form the boundary conditions for the solution.

In experimental measurements, these perturbative corrections are incorporated by rescaling the value of  $g_1$  to the average  $Q^2$  of the experiment. This rescaling procedure relies on the assumption that the asymmetry  $g_1(x)/F_1(x)$  satisfies exact Bjorken scaling, i.e. that the  $Q^2$ -dependence of  $g_1$  coincides with that of  $F_1$ . Although this assumption is consistent with the present data (which cover only a small range of  $Q^2$  values at fixed  $x$ ), there is no theoretical justification for it. In particular, examination of the polarised and unpolarised splitting functions [6] shows that  $g_1(x)/F_1(x)$  should indeed show only a very

weak  $Q^2$  dependence in the large- $x$  region, where both structure functions are dominated by the valence quark content, as  $\Delta P_{qq}(x)$  and  $P_{qq}(x)$  are identical. In contrast to this, the splitting functions in the singlet sector, which dominates the small- $x$  behaviour of  $F_1$ , are different. The unpolarised  $P_{qq}(x)$  and  $P_{gg}(x)$  have a soft gluon singularity at  $x = 0$ , which causes the steep rise of  $F_1$  in the small- $x$  region. As this singularity is absent in the polarised splitting functions (soft gluon emission does not change the spin of the parent parton), one would expect the ratio  $|g_1(x)/F_1(x)|$  to decrease with increasing  $Q^2$ .

With the exact splitting functions

$$\begin{aligned}
\Delta P_{qq}^{(f)}(x) &= \frac{4}{3} \left[ 2 \frac{1}{(1-x)_+} - 1 - x + \frac{3}{2} \delta(1-x) \right] \\
\Delta P_{qg}^{(f)}(x) &= 2n_f \frac{1}{2} [2x - 1] \\
\Delta P_{gq}^{(f)}(x) &= \frac{4}{3} [2 - x] \\
\Delta P_{gg}^{(f)}(x) &= 3 \left[ 2 \frac{1}{(1-x)_+} + 2 - 4x + \frac{11}{6} \delta(1-x) \right] - \frac{n_f}{3} \delta(1-x)
\end{aligned} \tag{3}$$

it is not possible to find an analytic solution to (2) with realistic boundary conditions for the whole range of  $x$ . By restricting themselves to small values of  $x$  (although it is not *a priori* clear which values of  $x$  can be regarded as small), various authors have attempted to determine the asymptotic behaviour of  $g_1$  in the limit  $Q^2 \rightarrow \infty$ . One possible approach [4] is to assume that all the  $Q^2$  dependence is dominated by the evolution of the gluon, i.e. by  $\Delta P_{gg}(x)$ . This method gives successful predictions for the unpolarised structure functions, due to the  $1/x$  pole in the unpolarised  $P_{gg}$ . As this pole is not present in  $\Delta P_{gg}$ , the validity of this approach needs to be examined more carefully.

Another possible approach [7] to the asymptotic small- $x$  behaviour is to transform (3) into moment space and to expand around the rightmost singularity at  $N = 0$ :

$$\langle \Delta P \rangle_N = \frac{A}{N} + B + O(N) \Rightarrow \Delta P(x) \approx A + B\delta(1-x). \tag{4}$$

This procedure yields the following approximate splitting functions<sup>1</sup>:

$$\begin{aligned}
\Delta P_{qq}^{(l)}(x) &= \frac{4}{3} \left[ 1 + \frac{1}{2} \delta(1-x) \right] \\
\Delta P_{qg}^{(l)}(x) &= 2n_f \frac{1}{2} [-1 + 2\delta(1-x)] \\
\Delta P_{gq}^{(l)}(x) &= \frac{4}{3} [2 - \delta(1-x)] \\
\Delta P_{gg}^{(l)}(x) &= 3 \left[ 4 - \frac{13}{6} \delta(1-x) \right] - \frac{n_f}{3} \delta(1-x)
\end{aligned} \tag{5}$$

---

<sup>1</sup>Similar splitting functions containing only the residue at  $N = 0$  were studied in [8], giving qualitatively comparable results to [7]

With these simplified splitting functions, one can analytically solve (2) for asymptotic values of  $Q^2$  with realistic boundary conditions in the small- $x$  region. This approach is based on the fact that the behaviour of the parton distributions at small  $x$  is governed by the region around  $N = 0$  in moment space. This property can be understood from the  $N$ -singularity structure of the initial distributions: a logarithmic ( $\sim 1/x$ ) singularity coincides with a pole at  $N = 0$  in the moment transform, a power-like singularity of the form  $x^\alpha$  transforms into  $\Gamma(\alpha + N)$ , which has a singularity at  $N = -\alpha$  (see Fig. 1). It is important to notice, however, that the expansion around the  $N = 0$  pole in moment space agrees with the full splitting function only within a circle of unit radius (Fig. 1). Outside this circle, the series might still be convergent, but its value will be different from that given by the full splitting function. This especially affects the reliability of this approach for low values of  $\alpha$ . In the extreme case  $\alpha$  could approach  $-1$  giving rise to a pole close to the boundary of the circle of convergence.

In this letter, we examine the validity of analytical approaches to the small- $x$  behaviour of  $g_1$ . Section 2 contains a study of the evolution matrix on the right-hand side of (2). Its properties in the case of power-like ( $x^\alpha$ ) boundary conditions are discussed, using the full and the leading-pole expanded splitting functions. By examining the sensitivity of the evolution matrix to the form of the parton distributions in the large- $x$  region, we are able to assess when  $x$  can be regarded as small. In Section 3 we present an analytic solution of (2), which becomes exact for  $x \rightarrow 0$ . Finally, Section 4 contains some phenomenological implications and conclusions.

## 2 Study of the evolution matrix

Several qualitative features of the polarised parton densities can already be determined by inserting simple test distributions in the right-hand side of Eq. (2). The resulting elements of the evolution matrix determine the local change of the parton densities with increasing  $\ln(Q^2)$ . Furthermore, for  $Q^2/Q_0^2$  not too large one can approximate the solution of the Altarelli-Parisi equations by

$$\begin{aligned} \begin{pmatrix} \Delta\Sigma \\ \Delta G \end{pmatrix}(x, Q^2) &= \begin{pmatrix} \Delta\Sigma \\ \Delta G \end{pmatrix}(x, Q_0^2) \\ &+ \frac{\alpha_s(Q_0^2)}{2\pi} \int_x^1 \frac{dy}{y} \begin{pmatrix} \Delta P_{qq} & \Delta P_{qg} \\ \Delta P_{gq} & \Delta P_{gg} \end{pmatrix}(y) \begin{pmatrix} \Delta\Sigma \\ \Delta G \end{pmatrix}(x/y, Q_0^2) \ln\left(\frac{Q^2}{Q_0^2}\right) \end{aligned} \quad (6)$$

A realistic choice of test distribution is

$$t(x) = x^\alpha(1-x)^\beta \quad \text{with} \quad (-1 < \alpha < 0, \beta > 0), \quad (7)$$

which is similar to the analytic forms of the parton densities at  $Q_0^2$  used in recent fits to the polarised structure function data [7, 9]. The exponent  $\alpha$  determines the behaviour of

the distribution in the small- $x$  regime, whereas the large- $x$  behaviour is controlled by  $\beta$ . Variations of  $\beta$  should therefore not affect any predictions of the small- $x$  behaviour of the parton distributions. This property can be used to define the range of validity of these predictions, i.e. to indicate if  $x$  can be regarded as small or not.

The elements of the evolution matrix

$$A_{ij} = \int_x^1 \frac{dy}{y} \Delta P_{ij}(y) t\left(\frac{x}{y}\right) \quad (8)$$

can be computed analytically. The necessary integrals are given in Appendix A. Using the full splitting functions (3), we find<sup>2</sup>

$$\begin{aligned} A_{qq}^{(f)}(x) &= \frac{4}{3} \left[ 2A_1(x) - A_2(x) - A_3(x) + \frac{3}{2}A_4(x) \right] \\ A_{qg}^{(f)}(x) &= 3[-A_2(x) + 2A_3(x)] \\ A_{gq}^{(f)}(x) &= \frac{4}{3} [2A_2(x) - A_3(x)] \\ A_{gg}^{(f)}(x) &= 3 \left[ 2A_1(x) + 2A_2(x) - 4A_3(x) + \frac{3}{2}A_4(x) \right], \end{aligned} \quad (9)$$

while the leading-pole expanded [7] splitting functions of (5) yield

$$\begin{aligned} A_{qq}^{(l)}(x) &= \frac{4}{3} \left[ A_2(x) + \frac{1}{2}A_4(x) \right] \\ A_{qg}^{(l)}(x) &= 3[-A_2(x) + 2A_4(x)] \\ A_{gq}^{(l)}(x) &= \frac{4}{3} [2A_2(x) - A_4(x)] \\ A_{gg}^{(l)}(x) &= 3 \left[ 4A_2(x) - \frac{5}{2}A_4(x) \right]. \end{aligned} \quad (10)$$

A closer inspection of the  $A_{ij}$  shows that all of them diverge like  $x^\alpha$  as  $x \rightarrow 0$ . The behaviour in the limit  $x \rightarrow 0$  can therefore be written as

$$\lim_{x \rightarrow 0} A_{ij}(x) = a_{ij} x^\alpha. \quad (11)$$

Provided that both the initial quark singlet and the initial gluon distributions have power-like boundary conditions in the limit  $x \rightarrow 0$ , these most singular terms will dominate the right-hand side of (2). The replacement of the  $A_{ij}^{(f)}$  by the above expressions (11) in (2) should therefore enable us to find an analytic solution for  $\Delta\Sigma(x, Q^2)$  and  $\Delta G(x, Q^2)$ , which becomes exact for  $x \rightarrow 0$ . This exercise will be performed in the following section.

---

<sup>2</sup>For simplicity, we take  $n_f = 3$  throughout this study

The  $a_{ij}$  coefficients for the full and the leading-pole expanded splitting functions are *not* identical:

$$\begin{aligned}
a_{qq}^{(f)} &= \frac{4}{3} \left[ 2(-\psi(-\alpha) - \gamma_E) + \frac{1-2\alpha}{\alpha(1-\alpha)} + \frac{3}{2} \right] & a_{qq}^{(l)} &= \frac{4}{3} \frac{-2+\alpha}{2\alpha} \\
a_{qg}^{(f)} &= 3 \frac{1+\alpha}{\alpha(1-\alpha)} & a_{qg}^{(l)} &= 3 \frac{1+2\alpha}{\alpha} \\
a_{gq}^{(f)} &= \frac{4}{3} \frac{-2+\alpha}{\alpha(1-\alpha)} & a_{gq}^{(l)} &= \frac{4}{3} \frac{-2-\alpha}{\alpha} \\
a_{gg}^{(f)} &= 3 \left[ 2(-\psi(-\alpha) - \gamma_E) - \frac{2+2\alpha}{\alpha(1-\alpha)} + \frac{3}{2} \right] & a_{gg}^{(l)} &= 3 \frac{-8-5\alpha}{2\alpha}
\end{aligned} \tag{12}$$

Here  $\psi(x)$  is the usual psi (digamma) function [10].

Figure 2 shows the  $A_{ij}^{(f)}$  for  $\alpha = -0.25, -0.6$  and  $\beta = 4, 9$ , together with the approximate forms  $A_{ij}^{(l)}$  and the limits  $a_{ij}^{(f)} x^\alpha$ . This figure displays the following important features of the evolution matrix in the small- $x$  region:

- (i) Although the test distributions  $x^\alpha(1-x)^4$  and  $x^\alpha(1-x)^9$  differ by less than 5% for  $x \leq 0.01$ , the corresponding  $A_{ij}^{(f)}$  differ by up to a factor of 2 in the same range. This clearly demonstrates that even at  $x = 0.01$  and below the evolution is sensitive to the behaviour of the parton distributions in the large- $x$  region. The insensitivity of the  $A_{ij}^{(f)}$  to variations of  $\beta$  can furthermore be used to define whether  $x$  can be regarded as small. For example, by requiring  $A_{ij}^{(f)}$  to vary by less than 30% for all combinations in  $i$  and  $j$  and both values of  $\alpha$ , we find that only  $x \leq 0.001$  can be regarded as small, and the more conservative bound of less than 10% deviation yields  $x \leq 0.0001$ . It should therefore be clear that the mere knowledge of  $g_1$  at the lowest  $x$  values accessible with fixed-target experiments is insufficient to predict the asymptotic behaviour of  $g_1$  in the small- $x$  limit, as the behaviour of the parton distributions at these values of  $x$  is still closely correlated with the distributions in the large- $x$  region.
- (ii) The convergence of the  $A_{ij}^{(f)}$  towards  $a_{ij}^{(f)} x^\alpha$  improves for smaller values of  $\alpha$ . This behaviour just reflects the fact that  $A_{ij}^{(f)}$  contains, in addition to this leading term, less singular terms proportional to  $\ln(x)$ . In general, these lower  $|A_{ij}^{(f)}|$ . If  $t(x)$  is less singular than  $x^{-1/e}$ , the logarithmic terms are larger than the power-like terms for

$$x > x_0(\alpha) = \left( \frac{\omega(\alpha)}{\alpha} \right)^{\frac{1}{\alpha}} \tag{13}$$

where  $\omega(\alpha)$  is the branch of Lambert's  $\omega$ -function which satisfies  $\omega(-1/e) = -1$ . As  $x_0$  decreases very quickly with  $\alpha$  ( $x_0 \approx 10^{-15}$  for  $\alpha = -0.1$ ), the replacement  $A_{ij}^{(f)}(x) \rightarrow a_{ij}x^\alpha$ , although formally still correct, loses its meaning for values of  $\alpha$  close to 0 in any physically relevant region.

- (iii) While the  $A_{ij}^{(l)}$  resemble the  $A_{ij}^{(f)}$  for values of  $\alpha$  close to 0, they disagree for smaller  $\alpha$ . This feature becomes most striking for the  $A_{qg}$  (see Fig. 2). The full splitting functions [6] predict that a positive gluon polarisation in the small- $x$  region will always generate a negative contribution to the sea polarisation. In contrast, the leading-pole expanded splitting functions of [7] predict a *positive* sea polarisation, if the gluon polarisation  $\Delta G(x)$  is more singular than  $x^{-0.5}$ . This behaviour can be inferred from the  $\alpha$  dependence of the  $a_{ij}$  displayed in Fig. 3. The good agreement for higher values of  $\alpha$  is due to the fact that all leading contributions in  $\ln(x)$  are contained in the  $N = 0$  pole and hence are well approximated by the  $A_{ij}^{(l)}$ . As elaborated above, these contributions remain important for a finite range in  $x > x_0 > 0$ . The asymptotic predictions of [7] will therefore still approximate the full evolution, provided they are restricted to this finite range.
- (iv) The magnitude of  $A_{gg}$  is larger by a factor 3 than the magnitude of all the other terms, but  $A_{gg}$  is not more singular than any other contribution. Therefore, the small- $x$  estimate of Ref. [4] is quantitative at best, and should be expected to yield a less accurate prediction than the corresponding estimate of the unpolarised distributions.

	$N \leq -2$	$N = -1$	$N = 0$
$3/4 \Delta P_{qq}$	2	1	1
$1/3 \Delta P_{qg}$	0	2	-1
$3/4 \Delta P_{gq}$	0	-1	2
$1/3 \Delta P_{gg}$	2	-2	4

Table 1: Residues of the polarised splitting functions in  $N$ -moment space. The residues for all negative integers with  $N \leq -2$  are identical.

- (v) The agreement between leading pole expanded and full splitting functions is better for the  $A_{gq}$  and  $A_{gg}$  than it is for  $A_{qq}$  and  $A_{qg}$ . This feature can be understood from the relative magnitude of the residues in the corresponding splitting functions

(Table 1): the  $N = 0$  residue is dominant only in the  $P_{qq}$  and  $P_{gg}$  splitting functions, the other two splitting functions contain residues for  $N < 0$ , which are twice as big as the  $N = 0$  residue.

It should be clear from the above that the leading-pole expansion of Ref. [7] gives a reliable approximation to the evolution matrix in the small- $x$  region, provided that the initial distributions are significantly less singular than  $x^{1/e}$ . For more singular distributions, this approach results in a manifestly different evolution matrix and hence will yield a different small- $x$  behaviour of the polarised parton distributions.

### 3 Solution of the Altarelli-Parisi equations in the limit $x \rightarrow 0$

Provided both polarised singlet quark and gluon densities have power-like boundary conditions in the small- $x$  region,

$$\Delta\Sigma(x, Q_0^2) \sim x^{\alpha_q}, \quad \Delta G(x, Q_0^2) \sim x^{\alpha_G} \quad \text{with } -1 < \alpha_q, \alpha_G < 0, \quad (14)$$

one can find a solution of the Altarelli-Parisi equations which becomes exact in the limit  $x \rightarrow 0$  and has the form

$$\begin{aligned} \Delta q_{val}(x, Q^2) &= R_v(Q^2, Q_0^2) x^{\alpha_v} \\ \Delta\Sigma(x, Q^2) &= R_{qq}(Q^2, Q_0^2) x^{\alpha_q} + R_{qg}(Q^2, Q_0^2) x^{\alpha_G}, \\ \Delta G(x, Q^2) &= R_{gq}(Q^2, Q_0^2) x^{\alpha_q} + R_{gg}(Q^2, Q_0^2) x^{\alpha_G}. \end{aligned} \quad (15)$$

A detailed derivation of this solution and the explicit forms of the  $R$ -functions is given in Appendix B.

The above bounds on  $\alpha$  cover the whole theoretically allowed range: as the first moments of the distributions have to be finite, we find  $\alpha > -1$ . Furthermore, inspection of the singularity structure of the evolution equations (Fig. 1) shows that any initial distribution, which is finite in the small- $x$  region, will develop a logarithmic divergence due to the  $N = 0$  singularity of the splitting functions. The case of finite or logarithmic boundary conditions can be treated correctly with the leading-pole approximation – its asymptotics are discussed in [7]. In a previous analysis [9] of the experimental data on polarised structure functions we have found  $\alpha_q = \alpha_v \simeq -0.55$ . The experimental data used in this analysis were insufficient to determine  $\alpha_G$ , and therefore it was fixed to be 0. In contrast to this, more recent measurements at lower  $Q^2$  [3] favour  $\alpha_G < 0$ .

As we have neglected all contributions of order  $\ln(x)$  in the above solution, we expect it to be reliable only for  $x < x_0(\max(\alpha_q, \alpha_G))$ . In order to compare this approach with the leading pole expansion of Ref. [7] and the numerical solution of (2) with the full splitting



functions, we have evaluated the distributions for  $Q_0^2 = 4 \text{ GeV}^2$  and  $Q^2 = 100 \text{ GeV}^2$ , using  $n_f = 3$ ,  $\Lambda^{QCD} = 200 \text{ MeV}$  and the following initial distributions:

$$\begin{aligned}\Delta\Sigma(x, Q_0^2) &= N_q x^{\alpha_q} (1-x)^\beta \\ \Delta G(x, Q_0^2) &= N_G x^{\alpha_G} (1-x)^\beta \\ \Delta q_{val}(x, Q_0^2) &= N_{val} x^{\alpha_v} (1-x)^\beta.\end{aligned}\tag{16}$$

To illustrate the validity of the various approximations, we adopt the following parameter values:  $\alpha_q, \alpha_G, \alpha_v = -0.6, -0.25, \beta = 4, 9$ , and for simplicity we take  $N_q = N_g = N_v = 1$ .

Figures 4 (a), (b) and (c) show the behaviour of the gluon, singlet quark and valence quark distributions respectively, at small  $x$  and  $Q^2 = 4, 100 \text{ GeV}^2$ . The initial distributions  $x^\alpha(1-x)^4$  are indicated as solid lines.

Starting with the gluon distribution (Fig. 4(a)), we see that for  $x < 10^{-2}$ , the leading-pole approximation to the splitting functions (dotted lines) gives excellent agreement with the full evolution (dashed line), especially for values of  $\alpha_q, \alpha_G$  close to 0. This is consistent with the agreement between the corresponding  $A_{gg}$  functions shown in Fig. 2 and can be understood from the  $N = 0$  dominance in the  $\Delta P_{gq}$  and  $\Delta P_{gg}$  splitting functions. In contrast, the  $x^\alpha$  approximation (short-dashed line) significantly overestimates the evolution in the  $x$  range shown, especially for  $\alpha_q, \alpha_G$  close to 0. Convergence of this approach can only be observed at even smaller values of  $x$ . Note, however, the sensitivity to the large- $x$  behaviour. While both the dotted and the dashed lines are computed with  $\beta = 4$ , the dot-dashed curve corresponds to full splitting function evolution for  $\beta = 9$ , i.e. a softer large- $x$  distribution. Evidently there is a significant sensitivity to the behaviour at large  $x$  even for  $x$  values as small as  $O(10^{-3})$ . This casts doubt on the idea of using data on the evolution of the small- $x$  structure functions alone to determine the gluon distribution.

For the singlet quark distribution (Fig. 4(b)) the situation is rather different. Here the leading-pole approximation *overestimates* the evolution at small  $x$ . This is readily understood from the behaviour of the corresponding  $A_{qq}$  and  $A_{qg}$  functions in Fig. 2, both of which are systematically more positive for the leading-pole splitting functions. In fact we see that for  $\alpha_q = -0.25$  and  $\alpha_G = -0.6$ , the full evolution gives a negative singlet distribution at small  $x$ , whereas the leading pole splitting functions give a positive distribution. Notice also that the evolution is less sensitive to the large- $x$  behaviour (compare the dashed and dot-dashed curves which correspond to  $\beta = 4, 9$  respectively) than for the gluon distribution. For  $\alpha_q = \alpha_G = -0.6$ , the  $x^\alpha$  approximation is quite reasonable, and certainly better than the leading-pole approximation. However the opposite is true when both  $\alpha_q, \alpha_G$  are close to 0.

Finally, Fig. 4(c) compares the valence quark evolution in the various approximations. This depends only on  $\Delta P_{qq}$ , and so the behaviour here is a direct reflection of the corresponding  $A_{qq}$  shown in Fig. 2. In particular, for  $\alpha_q = -0.6$  the  $x^\alpha$  approximation is very good, while the leading-pole approximation overestimates the evolution at all  $x$  values

shown. For less singular small- $x$  behaviour ( $\alpha_q = -0.25$ ), however, both approximations reproduce the full evolution, the leading-pole approximation showing slightly better convergence for  $x > O(10^{-4})$ .

In practice, the normalisations of the singlet quark and gluon distribution,  $N_q$  and  $N_G$ , will not be the same. As the evolution of the gluon density is dominated by the gluon-to-gluon splitting, it will be almost unaffected by changes of  $N_q$ . Only if  $N_q$  is one or more orders of magnitude larger than  $N_G$ , will the impact of quark-to-gluon splitting become visible. More drastic effects of a change in the relative normalisation can be expected for the quark singlet distribution, as contributions from quark-to-quark and gluon-to-quark splitting have the same magnitude but opposite signs (cf. Fig. 3). Therefore, a relative increase of  $N_G$  yields a faster evolution of the quark distribution to negative values.

The convergence properties of the different analytic approaches are almost unaffected by changes in the normalisation. Only for  $N_G \gg N_q$  do we find that convergence of the  $x^\alpha$  approximation to the singlet distribution sets in for smaller values of  $x$ . This simply reflects an increased impact of the gluon-to-gluon splitting.

## 4 Conclusions

In this letter we have studied the feasibility of two different analytic approaches to the evolution of polarised parton densities at small  $x$ , finding that none of these approaches is able to give reliable predictions for the whole theoretically allowed range of boundary conditions in the small- $x$  region. In the leading-pole expansion [7, 8], the full splitting functions  $\Delta P_{ij}$  are replaced by the leading terms of their Laurent series around  $N = 0$ . As this approach correctly reproduces all terms proportional to  $\ln x$  generated in the evolution, it is found to be in good agreement with the full evolution if the initial quark and gluon distributions are less singular than  $x^{-1/e}$ . For more singular boundary conditions, only the gluon distribution is reproduced correctly, in particular the quark distribution is overestimated. Keeping only terms with powerlike singularities in the evolution equation, we were able to derive an exact solution of this equation in the limit  $x \rightarrow 0$ . As we have neglected all logarithmic terms in this approach, its convergence is best for boundary conditions of quark and gluon distributions more singular than  $x^{-1/e}$ . For less singular boundary conditions, this approach still converges towards the full solution, but its predictions are far away from the full solution for any realistic experimental value of  $x$ .

We have also shown that the evolution of the polarised gluon distribution is sensitive to the shape of this distribution in the large- $x$  region. This observation raises doubts on the possibility of determining the gluon polarisation from the evolution of  $g_1$  in the small- $x$  region. It furthermore demonstrates the need for complementary measurements of  $\Delta G(x)$  (e.g. from  $J/\Psi$ -production or direct- $\gamma$  measurements).

We have seen that the effects of the evolution on the quark distributions in the small- $x$  region are rather small, as the quark-to-quark and the gluon-to-quark splitting contribute with opposite signs. The gluon distribution is indeed rising with increasing  $Q^2$ , but only contributes to  $g_1$  at order  $\alpha_s(Q^2)$ . Bearing in mind that  $\Delta G$  contributes with a negative coefficient function to  $g_1$ , one expects that  $g_1$  will become negative at small  $x$  for asymptotic values of  $Q^2$ , due to the gluonic contribution and the negative sea polarisation generated from  $g \rightarrow q\bar{q}$  splitting.

In general, the effects of the evolution on the polarised parton densities will be more moderate than the effects on the unpolarised densities. The assumption of approximate scaling for  $g_1(x)/F_1(x)$  in the small- $x$  region is therefore rather doubtful. It seems more realistic to assume approximate scaling for  $g_1(x)$  for the range of fixed-target experiments, due to the partial cancellation of quark and gluon evolution as explained above.

## Acknowledgements

Financial support from the UK PPARC (WJS), and from the Gottlieb Daimler- und Karl Benz-Stiftung and the Studienstiftung des deutschen Volkes (TG) is gratefully acknowledged. This work was supported in part by the EU Programme ‘‘Human Capital and Mobility’’, Network ‘‘Physics at High Energy Colliders’’, contract CHRX-CT93-0357 (DG 12 COMA).

## A Convolution integrals of the test distribution

For the test distribution

$$t(x) = x^\alpha(1-x)^\beta \quad \text{with} \quad (-1 < \alpha < 0, \beta > 0), \quad (17)$$

the convolution integrals

$$A_{ij} = \int_x^1 \frac{dy}{y} \Delta P_{ij}(y) t\left(\frac{x}{y}\right) \quad (18)$$

on the right-hand side of (2) can be expressed in an analytic form. From the explicit forms of the splitting functions given in (3) and (5), one sees that the required integrals are

$$\begin{aligned} A_1(x) &= \int_x^1 \frac{dy}{y} \frac{1}{(1-y)_+} \left(\frac{x}{y}\right)^\alpha \left(1 - \frac{x}{y}\right)^\beta \\ &= x^\alpha(1-x)^\beta [\ln(1-x) + \frac{\alpha + \beta + 1}{\beta + 1}(1-x) {}_3F_2(2 + \beta + \alpha, 1, 1; 2, 2 + \beta; (1-x)) \\ &\quad - \psi(\beta + 1) - \gamma_E] \end{aligned}$$

$$\begin{aligned}
A_2(x) &= \int_x^1 \frac{dy}{y} \left(\frac{x}{y}\right)^\alpha \left(1 - \frac{x}{y}\right)^\beta \\
&= (1-x)^{\beta+1} \frac{1}{\beta+1} {}_2F_1(1-\alpha, 1+\beta; 2+\beta; (1-x)) \\
A_3(x) &= \int_x^1 \frac{dy}{y} y \left(\frac{x}{y}\right)^\alpha \left(1 - \frac{x}{y}\right)^\beta \\
&= x(1-x)^{\beta+1} \left[ \frac{1}{1-\alpha} x^{\alpha-1} - \frac{\alpha+\beta}{(1-\alpha)(\beta+1)} {}_2F_1(1-\alpha, 1+\beta; 2+\beta; (1-x)) \right] \\
A_4(x) &= \int_x^1 \frac{dy}{y} \delta(1-y) \left(\frac{x}{y}\right)^\alpha \left(1 - \frac{x}{y}\right)^\beta \\
&= x^\alpha (1-x)^\beta.
\end{aligned} \tag{19}$$

All these functions diverge like  $x^\alpha$  as  $x \rightarrow 0$ , and the leading singular behaviour at small  $x$  is found to be

$$\begin{aligned}
A_1(x) &\xrightarrow{x \rightarrow 0} x^\alpha [-\psi(-\alpha) - \gamma_E] \\
A_2(x) &\xrightarrow{x \rightarrow 0} \frac{1}{-\alpha} x^\alpha \\
A_3(x) &\xrightarrow{x \rightarrow 0} \frac{1}{1-\alpha} x^\alpha \\
A_4(x) &\xrightarrow{x \rightarrow 0} x^\alpha.
\end{aligned} \tag{20}$$

## B Analytic solution of the Altarelli-Parisi equations for $x \rightarrow 0$

A solution of the Altarelli-Parisi evolution equations (2) can never be more singular at  $x = 0$  than the starting distributions. It follows that the most singular parts of the valence quark, singlet quark and gluon distributions can be obtained by inserting the following ansatz

$$\begin{aligned}
\Delta q_{val}(x, Q^2) &= R_v(Q^2, Q_0^2) x^{\alpha_v} \\
\Delta \Sigma(x, Q^2) &= R_{qq}(Q^2, Q_0^2) x^{\alpha_q} + R_{qg}(Q^2, Q_0^2) x^{\alpha_G}, \\
\Delta G(x, Q^2) &= R_{gq}(Q^2, Q_0^2) x^{\alpha_q} + R_{gg}(Q^2, Q_0^2) x^{\alpha_G}
\end{aligned} \tag{21}$$

into (2). Keeping only terms proportional to  $x^{\alpha_v}$ ,  $x^{\alpha_q}$  and  $x^{\alpha_G}$  on the right-hand side, we obtain the following evolution equations for the  $R$  coefficients ( $\beta_0 = 11 - 2/3n_f$ ):

$$\frac{\partial}{\partial \ln \alpha_s} R_v(Q^2, Q_0^2) = -\frac{2}{\beta_0} a_{qq}(\alpha_v) R_v(Q^2, Q_0^2)$$

$$\begin{aligned}
\frac{\partial}{\partial \ln \alpha_s} \begin{pmatrix} R_{qq} \\ R_{gq} \end{pmatrix} (Q^2, Q_0^2) &= -\frac{2}{\beta_0} \begin{pmatrix} a_{qq}(\alpha_q) & a_{qg}(\alpha_q) \\ a_{gq}(\alpha_q) & a_{gg}(\alpha_q) \end{pmatrix} \begin{pmatrix} R_{qq} \\ R_{gq} \end{pmatrix} (Q^2, Q_0^2) \\
\frac{\partial}{\partial \ln \alpha_s} \begin{pmatrix} R_{qg} \\ R_{gg} \end{pmatrix} (Q^2, Q_0^2) &= -\frac{2}{\beta_0} \begin{pmatrix} a_{qq}(\alpha_G) & a_{qg}(\alpha_G) \\ a_{gq}(\alpha_G) & a_{gg}(\alpha_G) \end{pmatrix} \begin{pmatrix} R_{qg} \\ R_{gg} \end{pmatrix} (Q^2, Q_0^2). \quad (22)
\end{aligned}$$

As we are interested in the asymptotic solution for the *full* splitting functions, all  $a_{ij}$  in the above are  $a_{ij}^{(f)}$ .

Introducing

$$\begin{aligned}
s &= \ln \left( \frac{\ln(Q^2/\Lambda^2)}{\ln(Q_0^2/\Lambda^2)} \right) \\
\omega_{\pm}(\alpha) &= \frac{1}{2} \left( a_{qq}(\alpha) + a_{gg}(\alpha) \pm \sqrt{(a_{qq}(\alpha) - a_{gg}(\alpha))^2 + 4a_{qg}(\alpha)a_{gq}(\alpha)} \right), \quad (23)
\end{aligned}$$

the general solution of these equations reads

$$\begin{aligned}
R_v(Q^2, Q_0^2) &= N_v \exp \left\{ \frac{2}{\beta_0} a_{qq}(\alpha_v) s \right\} \\
R_{qq}(Q^2, Q_0^2) &= R_{qq+}(Q_0^2) \exp \left\{ \frac{2}{\beta_0} \omega_+(\alpha_q) s \right\} + R_{qq-}(Q_0^2) \exp \left\{ \frac{2}{\beta_0} \omega_-(\alpha_q) s \right\} \\
R_{gq}(Q^2, Q_0^2) &= R_{gq+}(Q_0^2) \exp \left\{ \frac{2}{\beta_0} \omega_+(\alpha_q) s \right\} + R_{gq-}(Q_0^2) \exp \left\{ \frac{2}{\beta_0} \omega_-(\alpha_q) s \right\} \\
R_{qg}(Q^2, Q_0^2) &= R_{qg+}(Q_0^2) \exp \left\{ \frac{2}{\beta_0} \omega_+(\alpha_G) s \right\} + R_{qg-}(Q_0^2) \exp \left\{ \frac{2}{\beta_0} \omega_-(\alpha_G) s \right\} \\
R_{gg}(Q^2, Q_0^2) &= R_{gg+}(Q_0^2) \exp \left\{ \frac{2}{\beta_0} \omega_+(\alpha_G) s \right\} + R_{gg-}(Q_0^2) \exp \left\{ \frac{2}{\beta_0} \omega_-(\alpha_G) s \right\}, \quad (24)
\end{aligned}$$

where the  $R_{ij\pm}(Q_0^2)$  are determined by the boundary conditions at  $Q_0^2$ . As we assume that the initial distributions for the quark singlet and the gluon have the form

$$\Delta \Sigma(x, Q_0^2) = N_q x^{\alpha_q}, \quad \Delta G(x, Q_0^2) = N_G x^{\alpha_G}, \quad (25)$$

these constants are determined to be

$$\begin{aligned}
R_{qq+}(Q_0^2) &= \frac{\omega_+(\alpha_q) - a_{gg}(\alpha_q)}{\omega_+(\alpha_q) - \omega_-(\alpha_q)} N_q, & R_{qq-}(Q_0^2) &= -\frac{\omega_-(\alpha_q) - a_{gg}(\alpha_q)}{\omega_+(\alpha_q) - \omega_-(\alpha_q)} N_q, \\
R_{gq+}(Q_0^2) &= \frac{a_{qg}(\alpha_q)}{\omega_+(\alpha_q) - \omega_-(\alpha_q)} N_q, & R_{gq-}(Q_0^2) &= -\frac{a_{qg}(\alpha_q)}{\omega_+(\alpha_q) - \omega_-(\alpha_q)} N_q, \\
R_{qg+}(Q_0^2) &= \frac{a_{qg}(\alpha_G)}{\omega_+(\alpha_G) - \omega_-(\alpha_G)} N_g, & R_{qg-}(Q_0^2) &= -\frac{a_{qg}(\alpha_G)}{\omega_+(\alpha_G) - \omega_-(\alpha_G)} N_g, \\
R_{gg+}(Q_0^2) &= \frac{\omega_+(\alpha_G) - a_{qq}(\alpha_G)}{\omega_+(\alpha_G) - \omega_-(\alpha_G)} N_g, & R_{gg-}(Q_0^2) &= -\frac{\omega_-(\alpha_G) - a_{qq}(\alpha_G)}{\omega_+(\alpha_G) - \omega_-(\alpha_G)} N_g. \quad (26)
\end{aligned}$$

## References

- [1] J. Ellis and R.L. Jaffe, Phys. Rev. **D9** (1974) 1444, erratum **D10** (1974) 1669.
- [2] SLAC-Yale collaboration: M.J. Alguard et al, Phys. Rev. Lett. **37** (1976) 1261; G. Baum et al., Phys. Rev. Lett. **45** (1980) 2000; **51** (1983) 1135.  
EMC collaboration: J. Ashman et al., Nucl. Phys. **B328** (1989) 1.  
SLAC-E142 collaboration: D.L. Anthony et al., Phys. Rev. Lett. **71** (1993) 959.  
SMC collaboration: B. Adeva et al., Phys. Lett. **B302** (1993) 553, D. Adams et al., Phys. Lett. **B329** (1994) 399.
- [3] SLAC-E143 collaboration: K. Abe et al, Phys. Rev. Lett. **74** (1995) 346; **75** (1995) 25.
- [4] F.E. Close and R.G. Roberts, Phys. Lett. **B336** (1994) 257.
- [5] S.D. Bass and P.V. Landshoff, Phys. Lett. **B336** (1994) 537.
- [6] G. Altarelli and G. Parisi, Nucl. Phys. **B126** (1977) 298.
- [7] R.D. Ball, S. Forte and G. Ridolfi, Nucl. Phys. **B444** (1995) 287.
- [8] A. Berera, Phys. Lett. **B293** (1992) 445.
- [9] T. Gehrmann and W.J. Stirling, Z. Phys. **C65** (1995) 461.
- [10] See for example M. Abramowitz and I.A. Stegun, *Handbook of Mathematical Functions*, National Bureau of Standards Applied Mathematics Series 55 (1964).

## Figure Captions

**Figure 1** Singularity structure of the evolution equations in the complex  $N$ -moment plane. Dots ( $\bullet$ ) denote the poles of the splitting functions, and the cross ( $\times$ ) indicates the small- $x$  singularity of the initial distribution. The leading-pole expansion only converges to the splitting function in the unit circle around the origin.

**Figure 2** Elements of the splitting matrix for the test distribution  $x^\alpha(1-x)^\beta$ . Solid line: full splitting functions for  $\beta = 4$ , long-dashed line: same for  $\beta = 9$ , short-dashed line: most singular  $x^\alpha$  contribution, dotted line: leading-pole expanded splitting functions for  $\beta = 4$ , dot-dashed line: same for  $\beta = 9$ . For better visibility, all elements are multiplied by  $x$ .

**Figure 3** Coefficients of the most singular pieces in the splitting matrix for the full (left) and the leading-pole expanded (right) splitting functions. Solid line:  $a_{qq}$ , long-dashed line:  $a_{qg}$ , short-dashed line:  $a_{gq}$ , dotted line:  $a_{gg}$ .

**Figure 4** Evolution of test distributions for gluons ( $x\Delta G(x, Q^2)$ ), (a), singlet quarks ( $x\Delta\Sigma(x, Q^2)$ ), (b) and valence quarks ( $x\Delta q_{val}(x, Q^2)$ ), (c) as described in the text. Solid line: starting distribution at 4 GeV<sup>2</sup>, long-dashed and dot-dashed line: evolved distributions at 100 GeV<sup>2</sup> for different large- $x$  behaviour at  $Q_0^2$ , short dashed line: result of  $x^\alpha$  approximation, dotted line: result of leading-pole approximation.

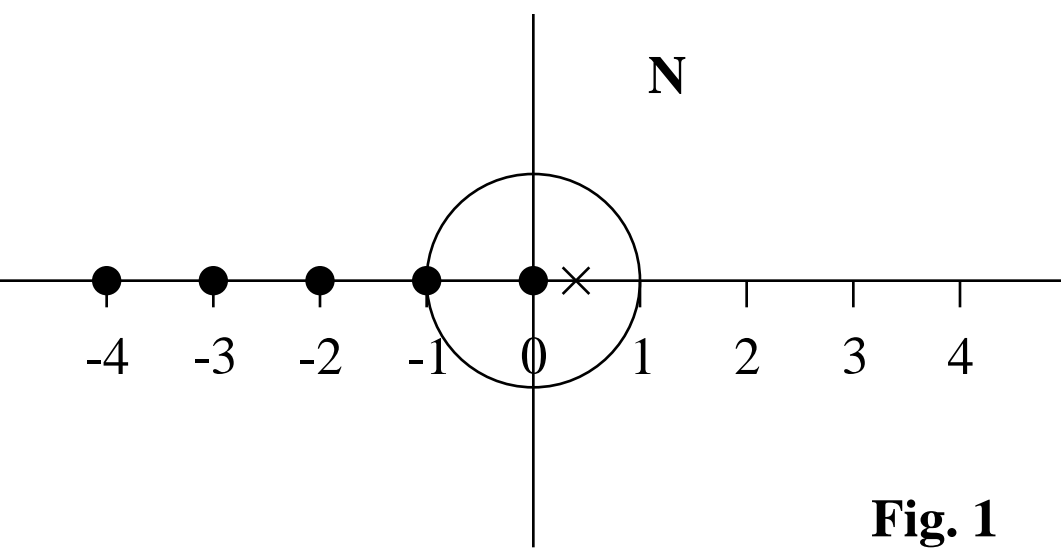


**Fig. 1**



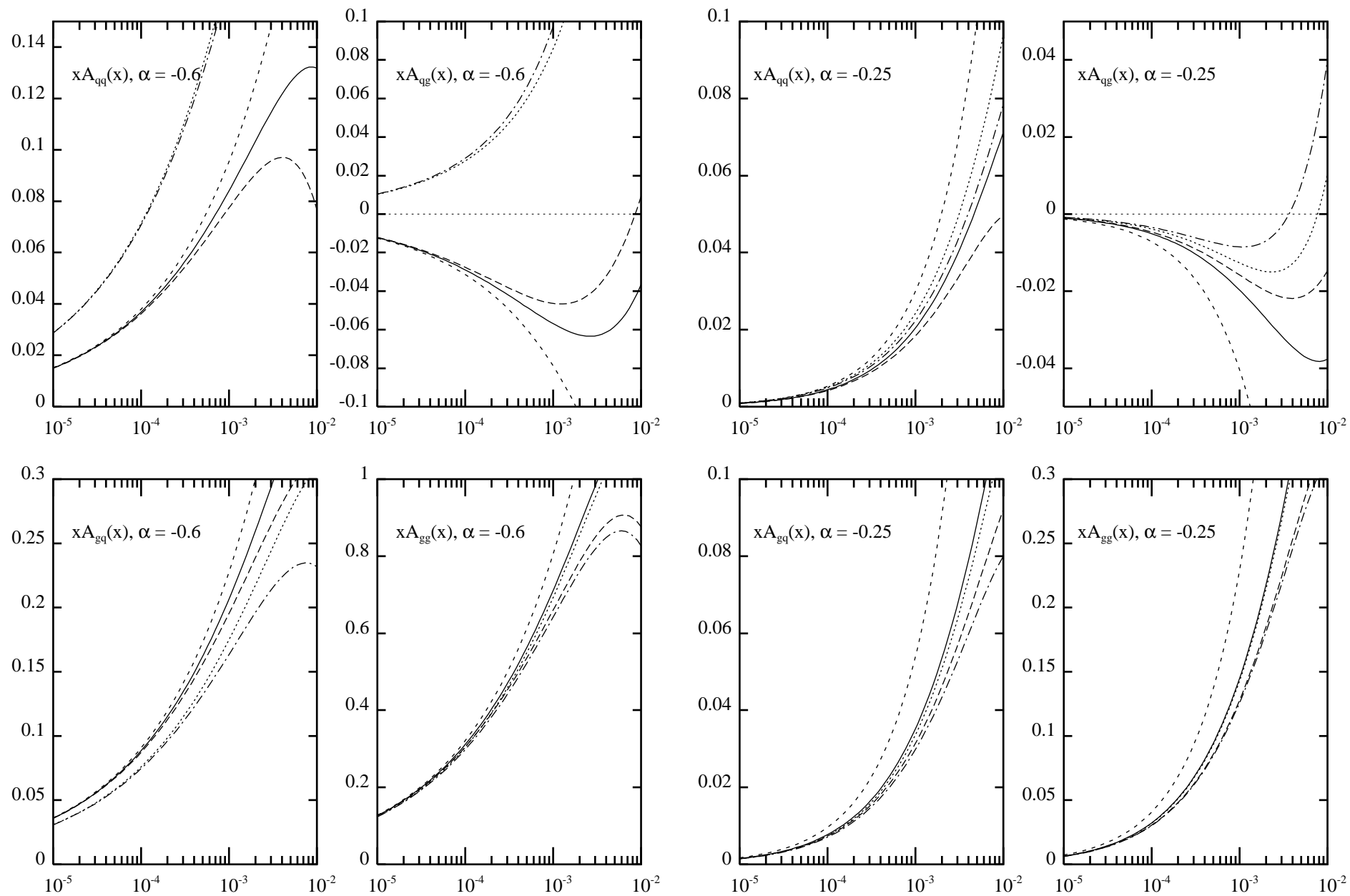


Fig. 2

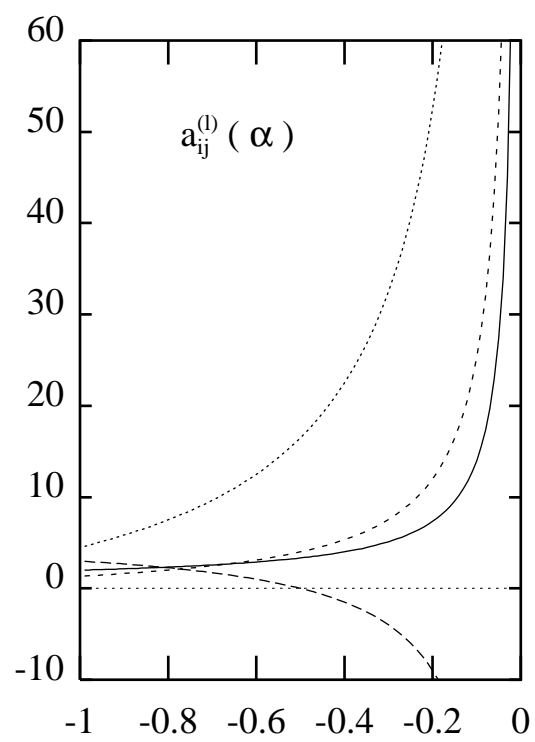
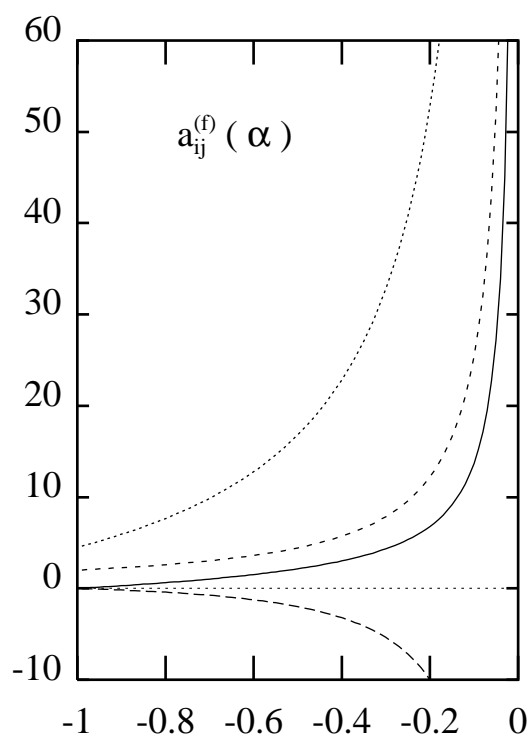


Fig. 3

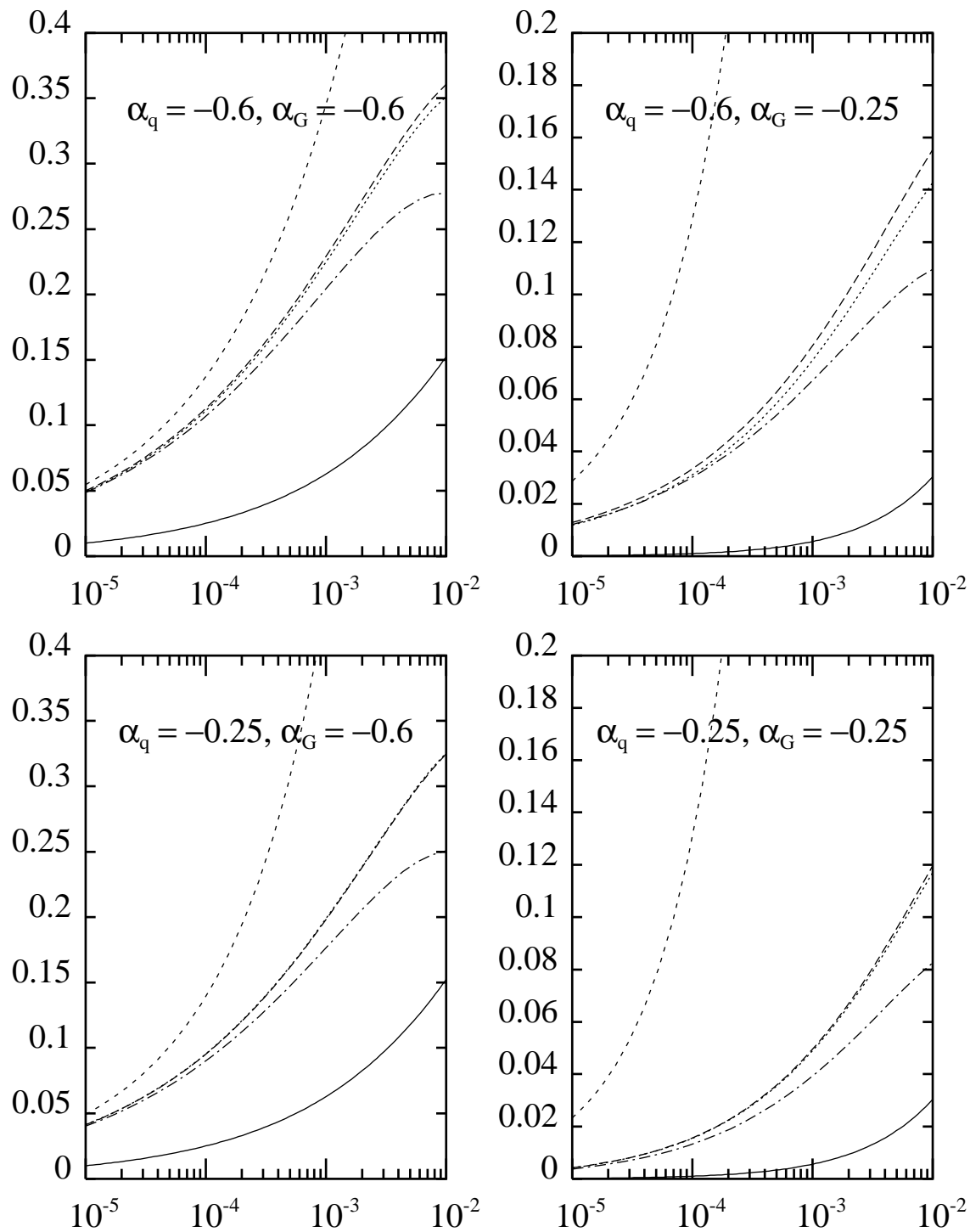


Fig. 4a

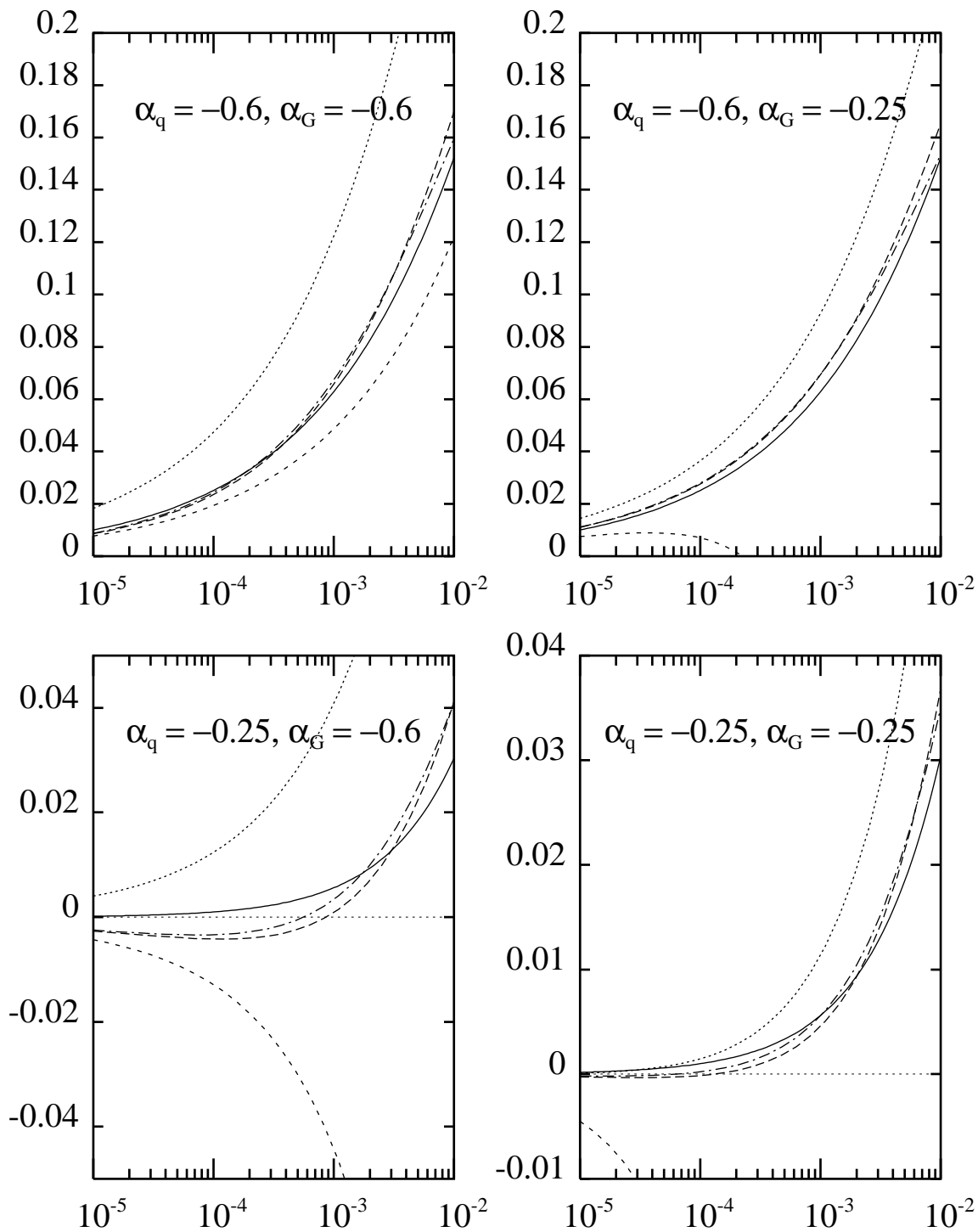


Fig. 4b

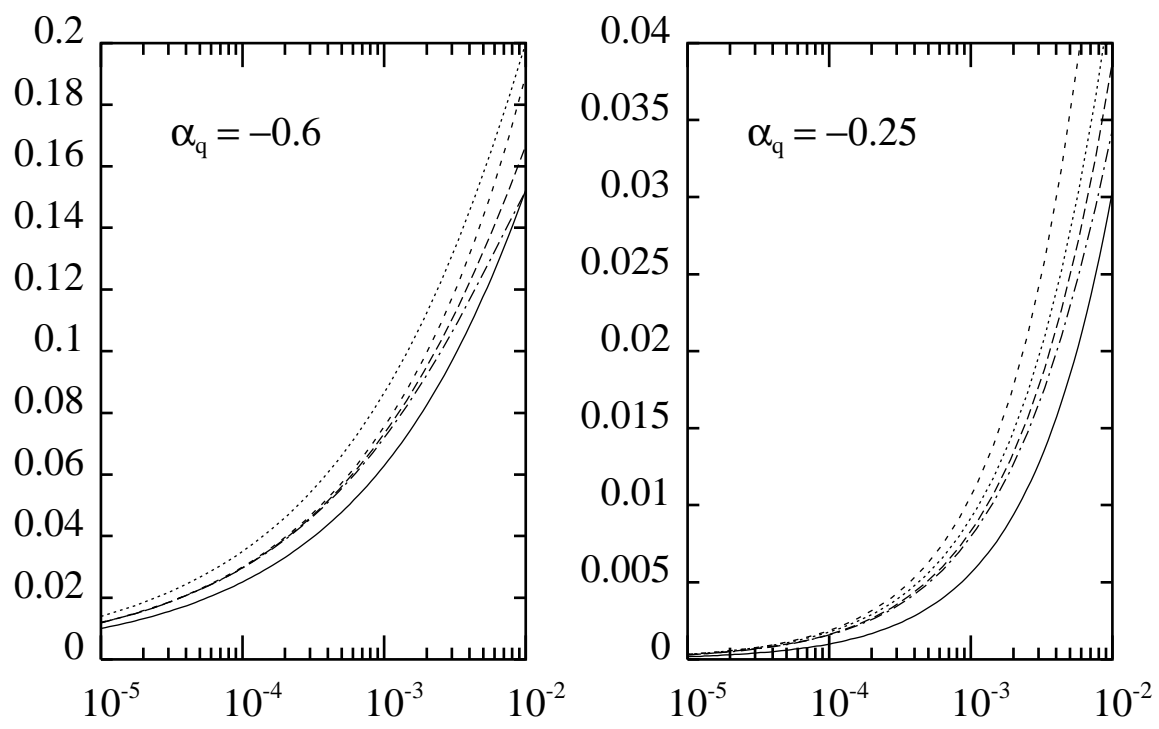


Fig. 4c